Azurin as a protein scaffold for a low-coordinate non-heme iron site with a small-molecule binding pocket

Matthew P. McLaughlin,[†] Marius Retegan,[§] Eckhard Bill,[§] Thomas M. Payne,[‡] Hannah S. Shafaat,[§] Salvador Peña,[†] Jawahar Sudhamsu,[‡] Amy A. Ensign,[†] Brian R. Crane,[‡] Frank Neese,[,§] and Patrick L. Holland*[,†]*

[†]Department of Chemistry, University of Rochester, Rochester, New York 14618

[‡]Department of Chemistry and Chemical Biology, Cornell University, Ithaca, New York 14853

[§] Max Planck Institute for Chemical Energy Conversion, Mülheim an der Ruhr, Germany

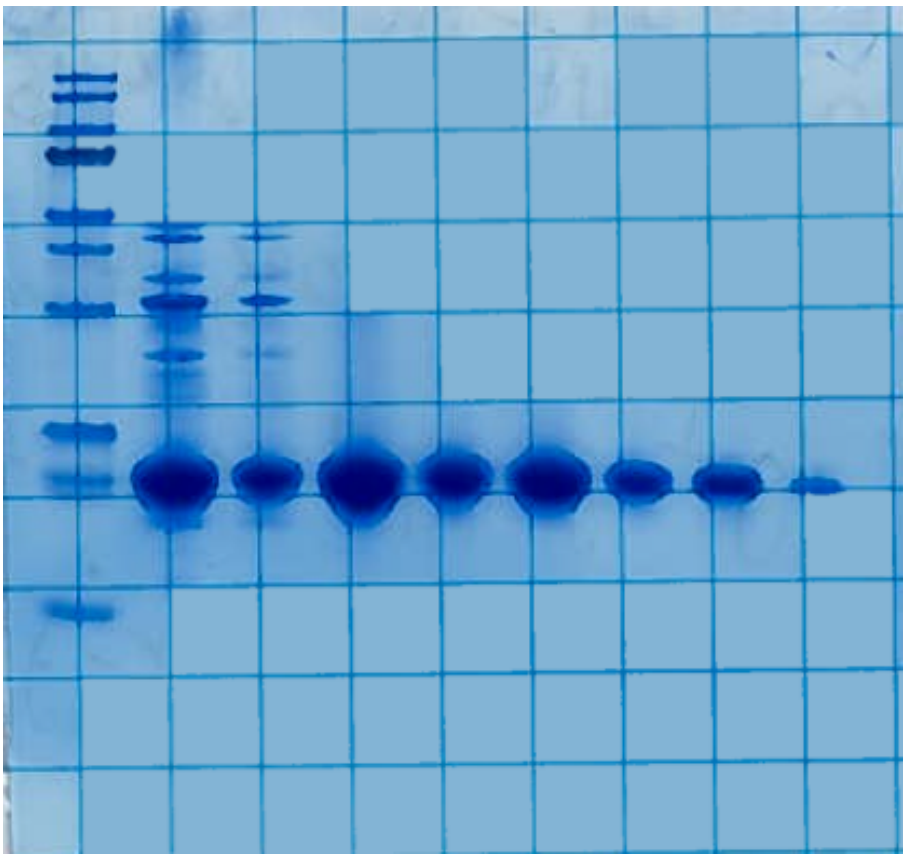

Figure S1. Gel electrophoresis of azurin during purification. From the left: (1) molecular weight ladder (2) 0% buffer B (early) (3) 0% buffer B (late) (4) 55% B buffer (early) (5) 55% buffer B (late) concentration after acidification (6) 65% buffer B (early) (7) 65% buffer B (late) (8) 85% buffer B (early) (9) 85% buffer B (late). Atomic absorption spectroscopy shows that before 85% buffer B the effluent of the ion exchange column is dominated by zinc azurin. Apo-azurin fractions for use in our experiments were collected starting from 85% buffer B (fractions 8 and 9). These samples had less than 2% zinc concentration relative to protein.

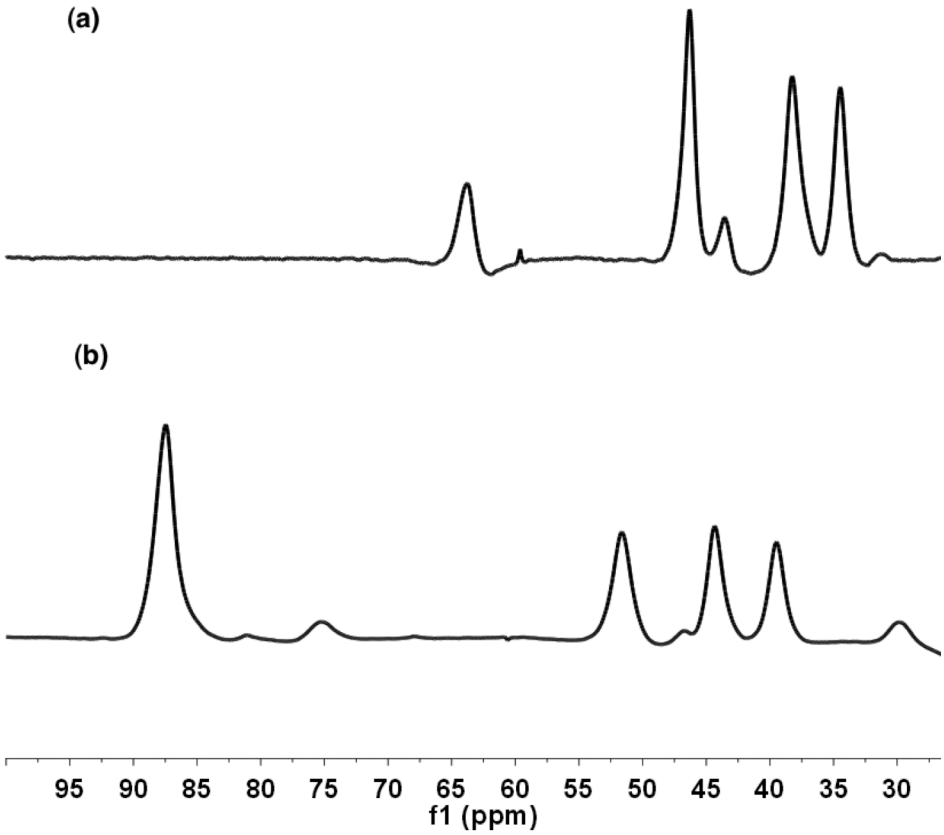

Figure S2. Downfield region of ^{1}H NMR spectra of 1.5 mM iron(II) azurins in 10% D_2O/H_2O. (a) Met121Ala variant. (b) Wild type.

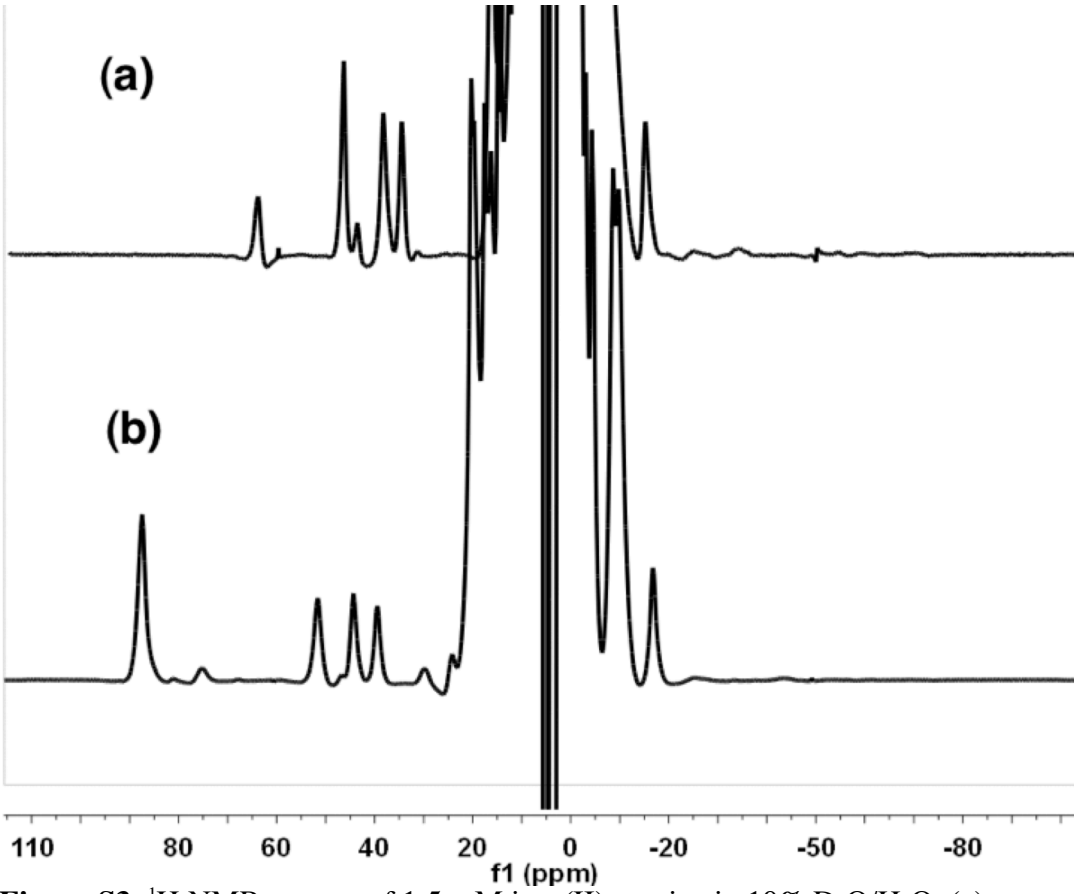

Figure S3. ^{1}H NMR spectra of 1.5 mM iron(II) azurins in 10% D_2O/H_2O. (a) Met121Ala variant. (b) Wild type.

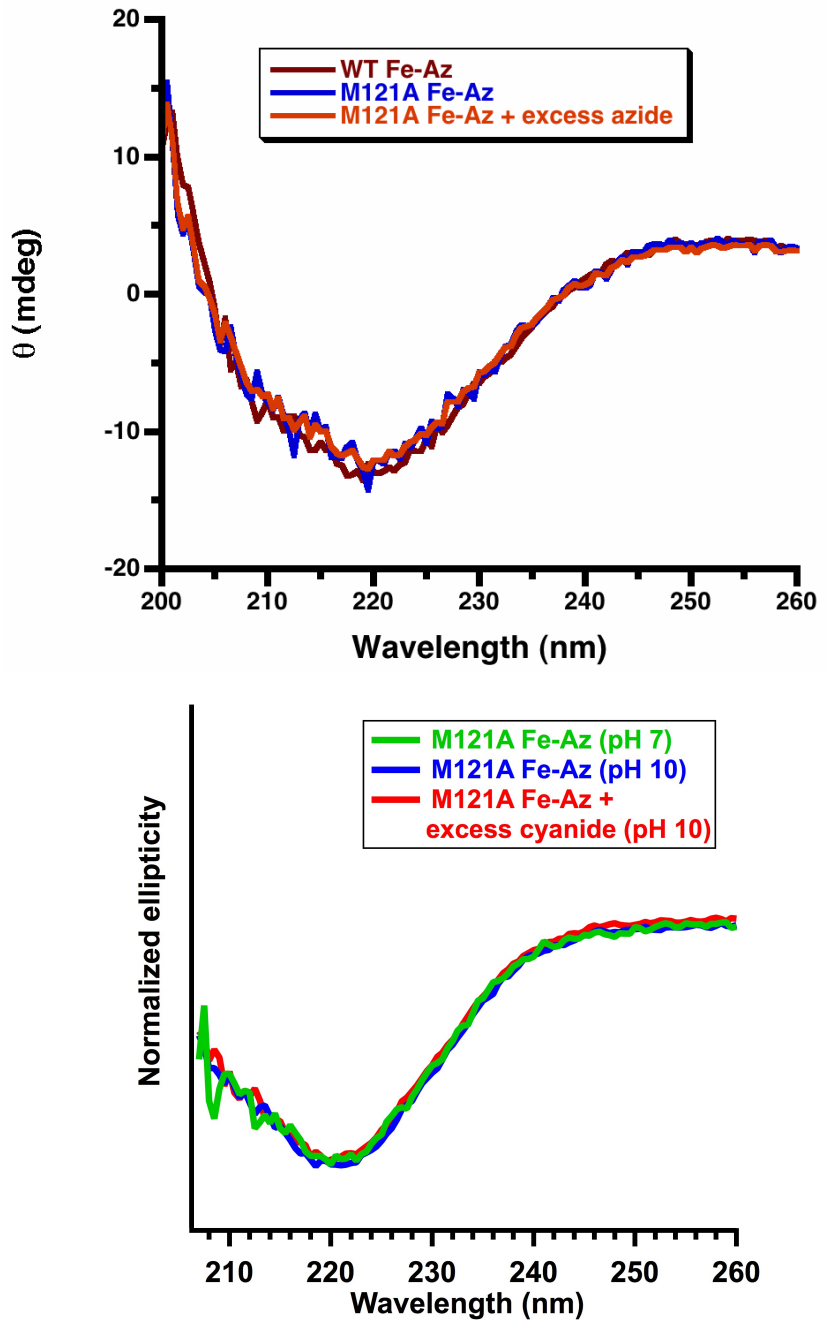

Figure S4. (Top) CD spectra of iron(II) azurin, iron(II)-M121A azurin, and the azide adduct of iron(II)-M121A azurin. (Bottom) CD spectra of iron(II)-M121A azurin at pH 7 (MOPS buffer), pH 10 (CAPS buffer), and with 50 mM KCN at pH 10 (CAPS buffer) after subtraction of appropriate blanks. The lower spectra are normalized to the peak intensity at 220 nm for direct comparison. Buffer and CN^- absorbance reduced the signal/noise ratio at $\lambda<207$ nm in the bottom spectra because of saturation of the PMT. Overall, the similarity of these spectra suggests that the mutation, the pH, and the cyanide binding do not lead to significant structural change within the protein.

Table S1. Anomalous diffraction at the high-energy side of the K-shell absorption edges for iron (1.61 Å) and zinc (1.27 Å). Values compared with the expected values for an iron substituted protein.

Wavelength (Å)	Observed f'' (e^-)	Theoretical f'' (e^-)	Occupancy (Chains B/C)
1.6082	3.35	3.39	0.35/0.35
1.2702	2.66	2.36	0.23/0.20

Figure S5. Tetrahedral geometry of the QM-only optimized wild type structure. Constrained atoms are marked with asterisks.

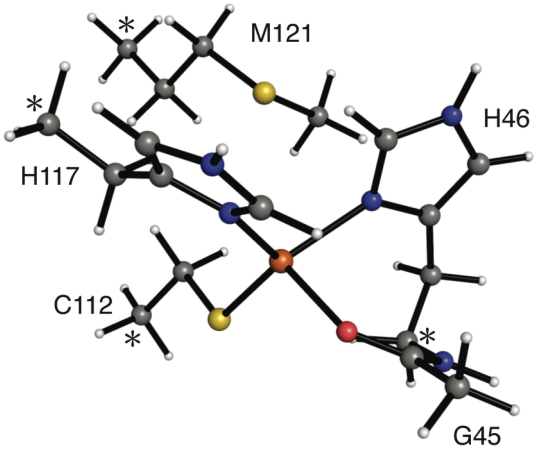

Table S2. Calculated energy and quadrupole splitting for different structures from a relaxed scan of Fe-O (Gly45) distance.

	Fe-O (Gly45)	ΔE (kcal/mol)	ΔE_Q (mm/s)
wt	2.00	1.13	-2.99
	2.05	0.47	-3.07
	2.10	0.10	-3.13
	2.15	0.00	-3.18
	2.20	0.07	-3.21
	2.25	0.34	-3.26
M121A mutant	2.00	0.73	-2.88
	2.05	0.20	-2.95
	2.10	0.00	-3.00
	2.15	0.08	-3.04
	2.20	0.32	-3.07
	2.25	0.69	-3.09

Table S3. Calculated ZFS parameters (cm^{-1}) by the DFT method, with the decomposition into spin-spin and spin-orbit contributions. As discussed in the text, these are far inferior to the CASSCF and NEVPT2 results.

	wt	mutant
D	3.9	3.7
E/D	0.2	0.1
D^{SS}	0.4	0.4
D^{SOC}	3.4	3.3
$\alpha \rightarrow \alpha$	0.1	0.1
$\beta \rightarrow \beta$	2.2	2.1
$\alpha \rightarrow \beta$	1.1	1.1
$\beta \rightarrow \alpha$	0	0

Table S4. QM optimized coordinates (Å) for the wild type structure.

C	27.126656	−7.854458	0.397476
C	25.888457	−8.061830	1.226185
O	25.212295	−7.055317	1.579423
N	25.563439	−9.325920	1.557331
C	24.426799	−9.651836	2.415126
C	23.230854	−10.245655	1.664128
C	22.803894	−9.401251	0.509347
C	22.474198	−9.775470	−0.772063
N	22.668697	−8.018180	0.613126
C	22.267167	−7.576468	−0.580808
N	22.138144	−8.611643	−1.438218
C	21.158573	−6.963550	6.549293
C	21.169942	−7.021435	5.009056
S	22.909860	−6.887570	4.349824
C	20.408664	−2.573761	2.636306
C	21.342649	−3.786600	2.629479
C	22.324677	−3.782767	1.506017
C	22.628721	−2.796701	0.594129
N	23.160127	−4.870513	1.262665
C	23.955550	−4.538909	0.241405
N	23.654081	−3.293975	−0.189536
C	16.352426	−6.128059	3.565008
C	17.807926	−6.405380	3.192948
C	18.039439	−6.299256	1.688938
S	19.682465	−6.890270	1.141776
C	19.487755	−8.667953	1.500065
Fe	23.198460	−6.715434	2.148479
H	27.798403	−7.172871	0.936397
H	26.844483	−7.365739	−0.545174

H	27.658704	−8.787276	0.175618
H	26.162937	−10.072220	1.217176
H	24.167352	−8.687138	2.868419
H	24.749545	−10.313625	3.231551
H	22.407591	−10.339181	2.392023
H	23.459610	−11.258789	1.304969
H	22.443215	−10.745817	−1.253118
H	22.066973	−6.542664	−0.833601
H	20.134461	−7.079980	6.933285
H	21.558578	−5.992714	6.876037
H	21.796237	−7.753775	6.971943
H	20.579169	−6.202885	4.577267
H	20.745840	−7.966001	4.640725
H	19.785875	−2.596022	3.541020
H	19.741225	−2.588569	1.762308
H	20.967436	−1.627085	2.637181
H	20.762983	−4.724478	2.575817
H	21.906833	−3.852702	3.575244
H	22.220128	−1.805786	0.440501
H	24.735709	−5.167046	−0.172055
H	16.221372	−6.207809	4.653741
H	15.668227	−6.848947	3.091568
H	16.042453	−5.117699	3.257897
H	18.084660	−7.410643	3.544477
H	18.477011	−5.701245	3.711566
H	17.980713	−5.252994	1.352535
H	17.277798	−6.866186	1.130051
H	20.350865	−9.187224	1.070495
H	18.569435	−9.046165	1.031374
H	19.464039	−8.858599	2.580146
H	21.831258	−8.543117	−2.403784
H	24.115787	−2.803425	−0.948809

Table S5. QM optimized coordinates (Å) for the Met121Ala mutant structure.

C	26.971526	−7.932736	0.153277
C	25.795712	−8.111856	1.072526
O	25.129393	−7.095700	1.419290
N	25.509482	−9.357300	1.490458
C	24.426800	−9.651840	2.415130
C	23.171894	−10.254539	1.765514
C	22.472486	−9.360622	0.789456
C	21.826543	−9.706455	−0.374852
N	22.308214	−7.990395	0.989637
C	21.578898	−7.532594	−0.030872
N	21.267692	−8.543807	−0.869149
C	21.158570	−6.963550	6.549290
C	21.234803	−7.005839	5.012395
S	23.008792	−6.801845	4.457720
C	20.408660	−2.573760	2.636310
C	21.334293	−3.792968	2.626552
C	22.303798	−3.798746	1.492325
C	22.565423	−2.838072	0.541928
N	23.160120	−4.874766	1.271850
C	23.923467	−4.562331	0.220081

N	23.584976	−3.340185	−0.245649
C	16.352430	−6.128060	3.565010
C	17.809846	−6.364992	3.157076
Fe	23.268563	−6.670845	2.253117
H	27.660912	−7.205872	0.603329
H	26.617408	−7.510854	−0.797462
H	27.508199	−8.868049	−0.044952
H	26.091547	−10.117733	1.150953
H	24.167350	−8.687140	2.868420
H	24.749550	−10.313630	3.231550
H	22.481055	−10.496102	2.590733
H	23.413430	−11.206480	1.270923
H	21.708510	−10.660398	−0.875195
H	21.290940	−6.498610	−0.182973
H	20.124961	−7.084157	6.902498
H	21.558580	−5.992710	6.876040
H	21.796240	−7.753780	6.971940
H	20.637496	−6.199399	4.566154
H	20.866094	−7.959872	4.611679
H	19.785880	−2.596020	3.541020
H	19.741230	−2.588570	1.762310
H	20.975905	−1.632613	2.637067
H	20.739999	−4.723048	2.584355
H	21.906185	−3.862850	3.567266
H	22.131414	−1.862176	0.363666
H	24.705531	−5.188920	−0.191379
H	16.221370	−6.207810	4.653740
H	15.668230	−6.848950	3.091570
H	16.018679	−5.122189	3.269015
H	20.718232	−8.460036	−1.719241
H	24.019225	−2.866616	−1.031563
H	17.938130	−6.301251	2.066093
H	18.167066	−7.354434	3.477810
H	18.473719	−5.613487	3.610552

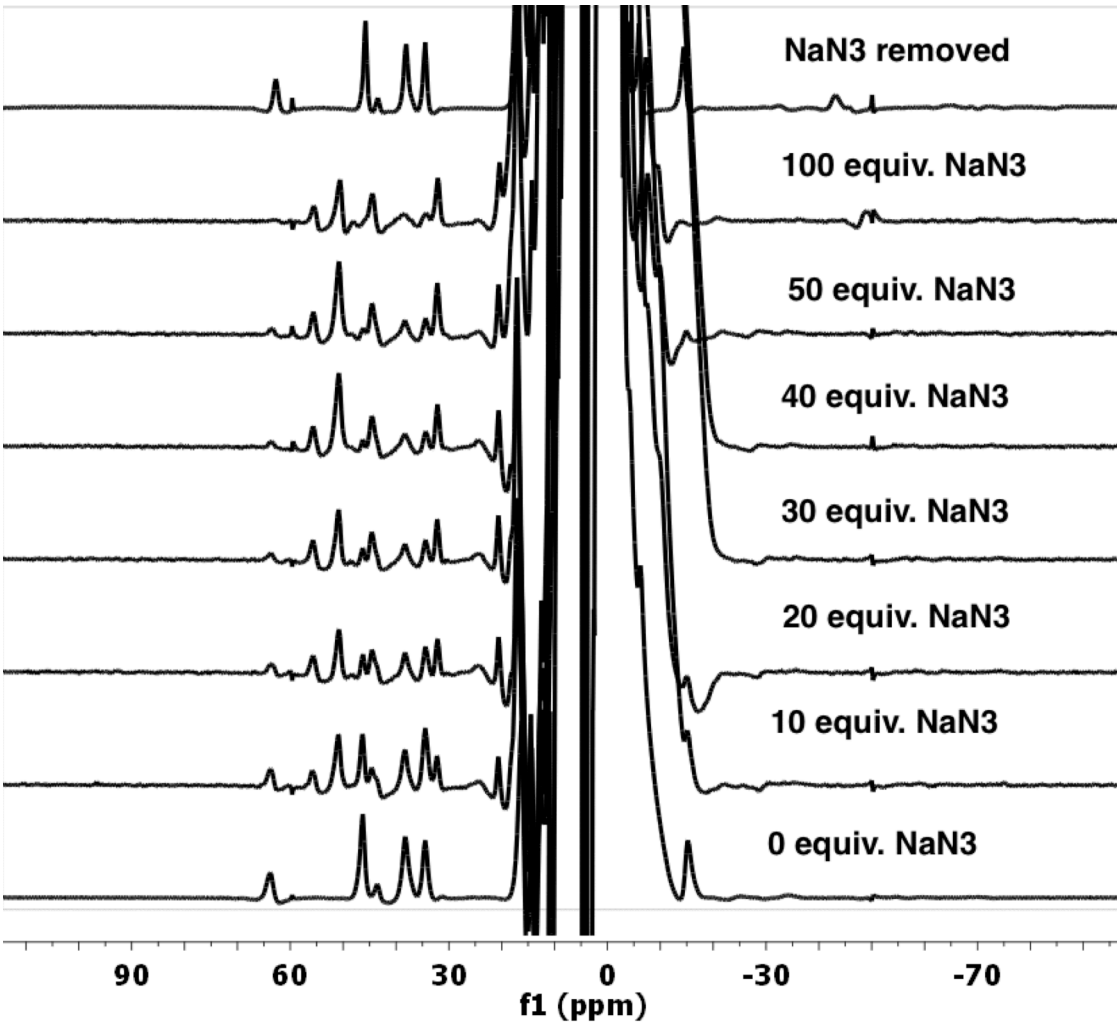

Figure S6. ^{1}H NMR spectra of 1.2 mM iron(II) azurin in 10% D_2O/H_2O with various concentrations of NaN_3 (0 to 120 mM). NaN_3 removed by three solvent exchanges using a Centricon concentrator (GE Healthcare, 3 kDa filter).

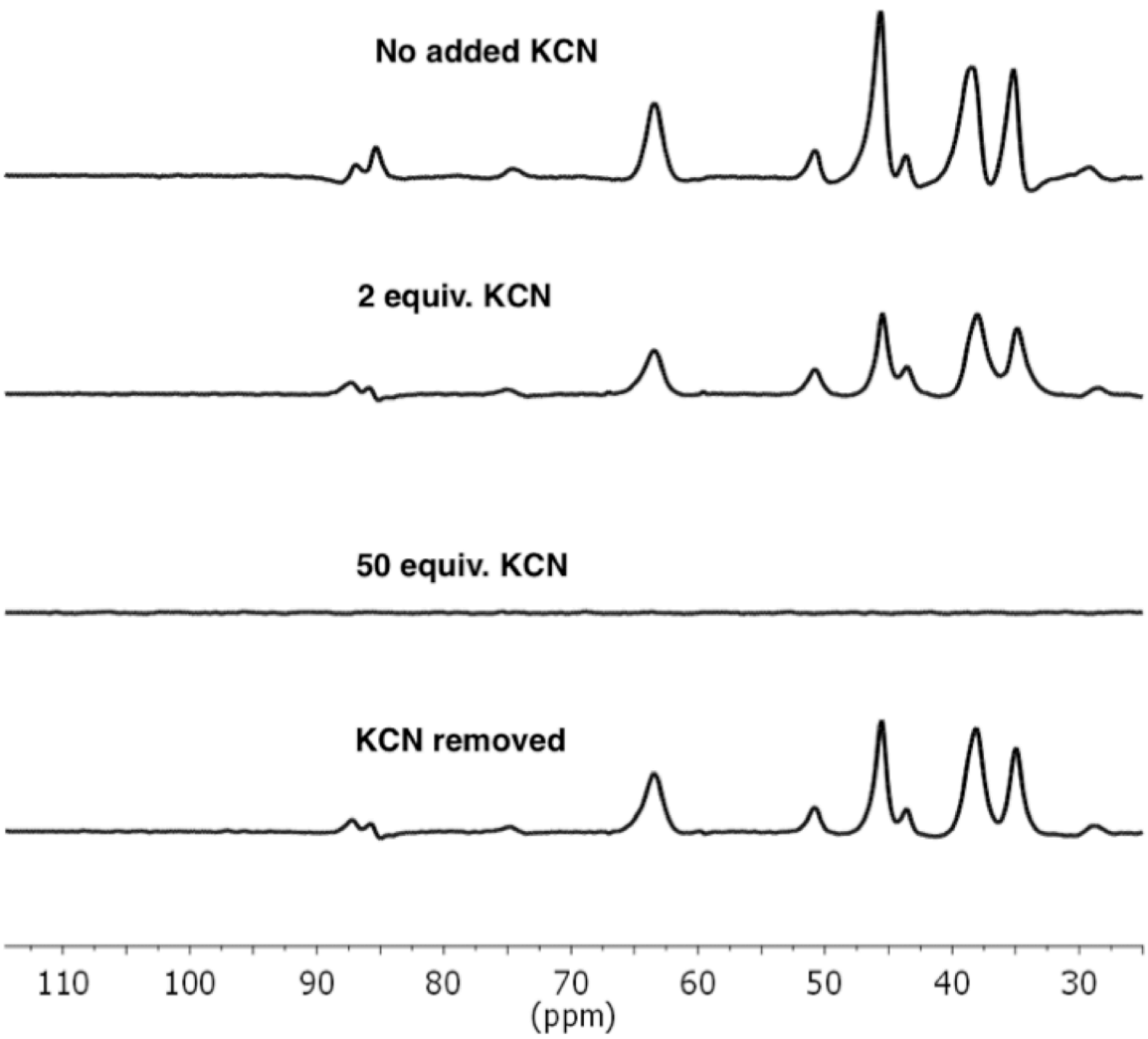

Figure S7. ^{1}H NMR spectra of 1.2 mM iron(II) azurin in 10% D_2O/H_2O with various concentrations of KCN (0 to 60 mM). The solutions were buffered at pH = 10 using CAPS. The KCN removed by 3 solvent exchanges using a Centricon concentrator (GE Healthcare, 3 kDa filter).

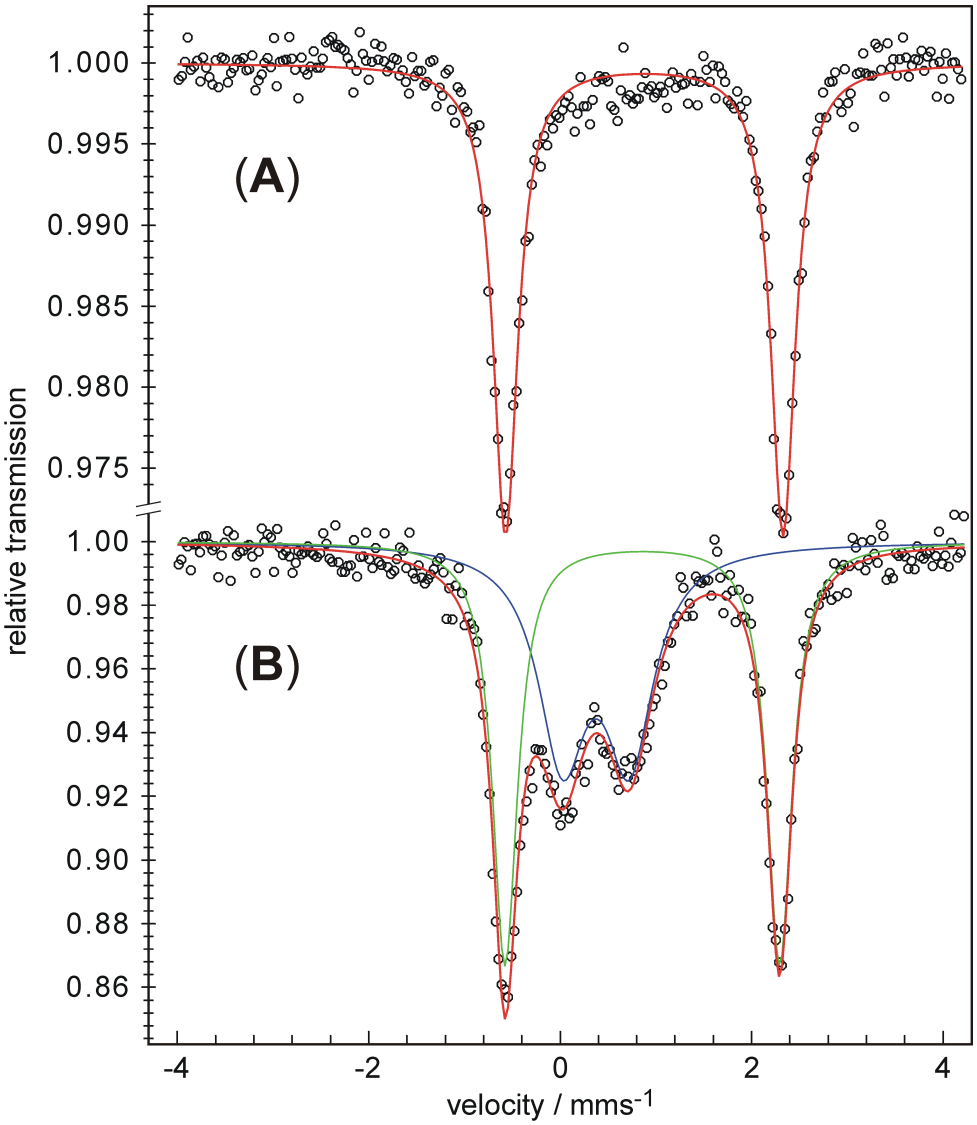

Figure S8. Zero-field Mössbauer spectra of (A) M121A ^{57}Fe azurin, and (B) M121A ^{57}Fe azurin + 50 mM KCN + 70 mM CAPS. The red line in (B) is the sum of two components: green (52%, IS 0.86, QS 2.87, LW 0.32, matches the spectrum in (A)) and blue (48%, IS 0.37, QS 0.70, LW 0.61). Due to the small volume, the pH was not carefully controlled during this addition of cyanide, and so the incomplete conversion to the low-spin cyanide adduct (blue component in B) may be the result of low [CN^-] in solution from partial loss to HCN.

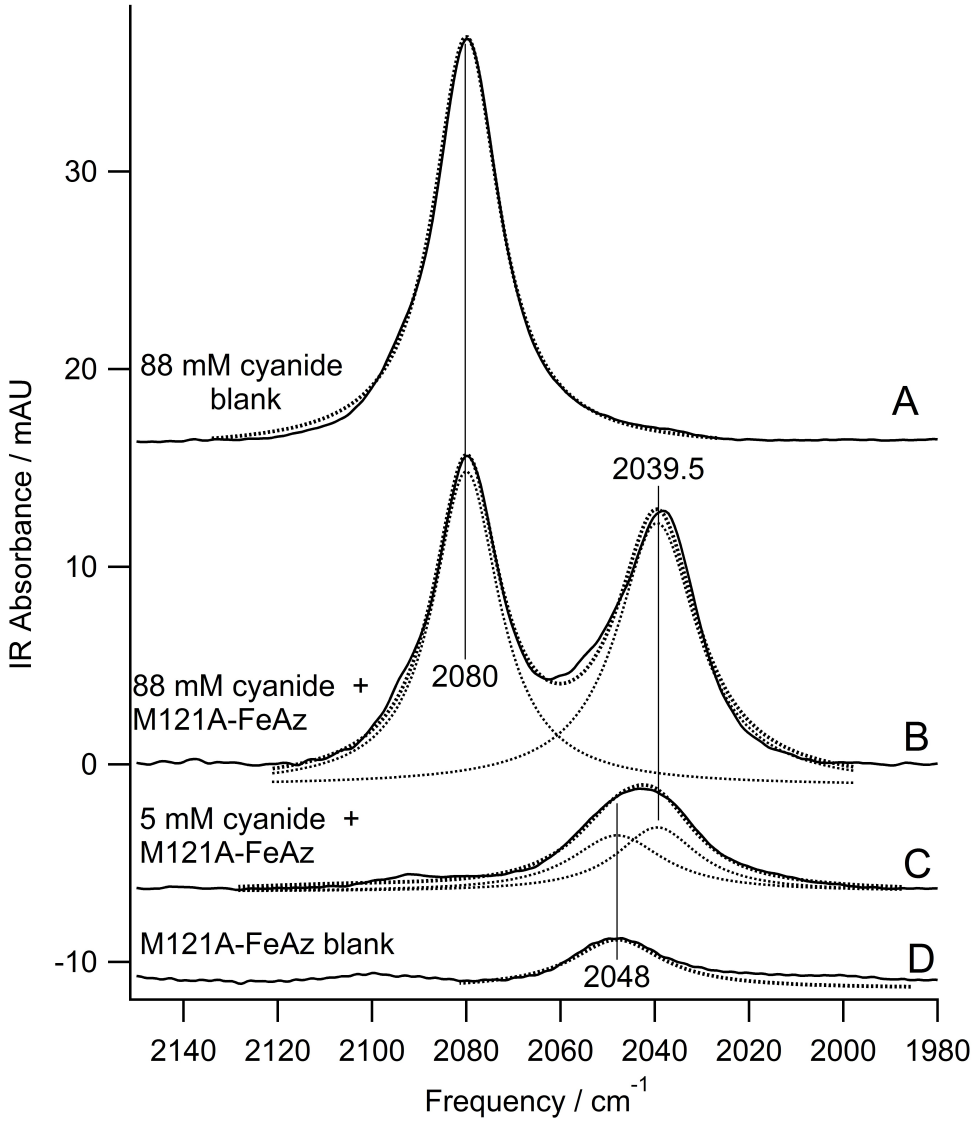

Figure S9. FTIR spectra from Figure 10 (solutions of 1.1 mM iron(II)-azurin in 100 mM CAPS buffer at pH 10), with decomposition of the signals into overlapping Lorentzian peaks. Peak frequency and linewidth constrained from single-component fits to A and D; bandwidth and frequency of the CN-bound FeAz obtained from the decomposition of B into A and an unknown component at 2039.5 cm^{-1}. The intensity of this peak indicates that the relative contributions of CN-bound protein and free protein in C are roughly 1:1. Note that the IR cross-section of the protein-CN adduct is much larger than that for free cyanide, consistent with metal binding.

Table S6. Crystallographic parameters. Data for outermost resolution shell given in parentheses.

Collection Parameters		
Wavelength (Å)	0.9202 Å	1.608 Å
Space group	$P2_12_12_1$	$P2_12_12_1$
Cell Parameters (Å, °)	a = 47.265, b = 98.030, c = 108.797, α=β=γ=90°	a = 47.309, b = 98.033, c =190.106, α=β=γ=90°
Resolution (Å)	40 – 1.78 (1.81 – 1.78)	43 – 2.20 (2.34 – 2.20)
No. of observations	89762	47265
No. of unique reflections	49440	26498
Completeness (%)	96.49	95.0
R_{sym} [a]	0.067 (0.227)	0.127 (0.340)
$I/\sigma(I)$	19.6 (5.6)	13.48 (5.54)
Refinement statistics		
Resolution range	40 – 1.78 (1.81 – 1.78)	43 – 2.20 (2.34 – 2.20)
R factor, %	23.3 (33.7)	24.5 (28.8)
R_{free}, %	26.1 (45.3)	27.7 (32.4)
Molecules / Asym unit	4	4
Residues	508	509
Atoms		
Protein	3868	3879
Solvent	422	166
Cofactor (Fe)	2	2
Mean B-values (Å^2)		
Overall	19.0	20.2
Main chain	17.5	19.6
Side chain	19.7	21.0
Solvent	24.7	18.3
Rmsd from ideal geometry		
Bonds	0.311 Å	0.312 Å
Angles	1.5°	1.5°
Ramachandran plot, %		
Most favored	90.2	89.1
Additionally allowed	9.8	10.9
Generously allowed	0.0	0.0
Disallowed	0.0	0.0
Missing residues	4	3

[a] $R_{sym} = \Sigma\Sigma_j |I_j - \langle I \rangle| / \Sigma\Sigma_j I_j$